A tether-less legged piezoelectric miniature robot using bounding gait locomotion for bidirectional motion

Hassan Hussein Hariri, Leonardus Adi Prasetya, Gim Song Soh, Shaohui Foong, Kevin Otto and Kristin Wood

***Abstract*— This paper describes the design and evaluation of a Legged Piezoelectric Miniature Robot (LPMR) propelled by standing wave locomotion where the vibrations of legs are similar to the bounding gait locomotion of animals. The LPMR comprises of one piezoelectric patch, a metal beam, two contact joints, two rigid legs and contains all necessary power electronics required for tether-less operation. Through analysis of the bending modes of vibrations and driving frequency, a forward and backward motion is achieved by choosing specific positions for the legs. At 100 V amplitude and without embedded mass, the LPMR with the weight of 6.27 g, the length of 50 mm, the width of 10 mm and the height of 1.5 mm achieves maximum linear speed of 246.5 mm/s for forward motion and 302 mm/s for backward motion. The LPMR is able to carry 100.8 g at a speed of 49.6 mm/s for forward motion and 87.9 mm/s for backward motion when applying 100 V amplitude. The LPMR has a blocking force of 12 mN for forward motion and 9.8 mN for backward motion at 100 V amplitude. An experimental characterization for the LPMR in terms of speed versus applied voltage, speed versus embedded mass and blocking force for different applied voltages is explored and evaluated in this study.**

I. INTRODUCTION

Piezoelectric materials are widely used in miniature mobile robots for actuation and sensing due to their abilities to generate forces when electric voltages are applied to them and vice versa to produce voltages when forces are applied to them [1], [2], [3], [4], [5], [6], [7], [8], [9], [10], [11]. They are characterized by high power to weight ratio which make them particularly suitable for meso or micro scale mobile robots [12]. The drawback of piezoelectric materials due to requirement of onboard high driven voltage is no longer a problem nowadays as many works are reported in literature to overcome this issue [13], [14], [15], [16], [17], [18] which now makes it possible to integrate onboard electronics at small scale for driving piezoelectric miniature robots. In this paper, we focus on Legged Piezoelectric Miniature Robots (LPMR's).

Two types of LPMR's exist in contemporary literature. The first type of LPMR's uses active legs where the legs are designed from piezoelectric materials [3], [19], [20], [21], [22]. The second type of LPMR's uses passive legs where piezoelectric actuators are used to create the motion of the passive legs [6], [16], [17], [18], [23], [24], [25], [26], [27], [28], [29], [30], [31], [32]. The LPMR described in this paper is subscribed in the second type where passive legs are used. It consists of one piezoelectric patch, a metal beam, two contact joints and two rigid legs as shown in Fig.1. The piezoelectric patch is bonded on the metal beam to form a unimorph piezoelectric actuator. The two rigid legs are attached to the metal beam through the contact joints. The purpose behind the use of a single piezoelectric patch in the design of the LPMR is to reduce the complexity of the onboard electronics, control and power consumption.

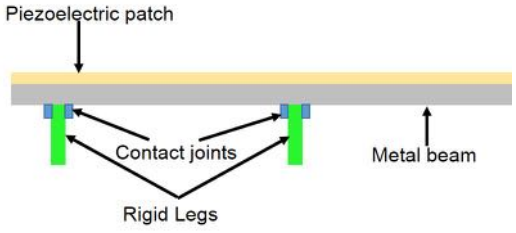

Fig. 1. Side view of LPMR structure

The LPMR in this research is easy to manufacture as it consists of a unimorph piezoelectric actuator that acts both as the base body and the excitation source for locomotion and two legs attached to it by rigid contact joints. Also, it doesn't require any linking mechanisms. We chose an asymmetrical design placement for legs to achieve a bidirectional motion. The legs of our LPMR are rigid and the motion direction is determined by the legs positions and the corresponding vibration modes of the beam. The design exploits the use of mechanical standing waves generated on the metal beam and transmitted to its legs to propel the LPMR forward and backward where the vibrations of legs are similar to the bounding gait locomotion of animals. In our proposed design, a forward and backward motion in one dimensional axis is determined by the mechanical design and placement of the legs of the LPMR, and two operating frequencies for both directions are selected by the designer as well. By simple change in the driving frequency, both forward and backward motion can be achieved on a smooth flat surfaces.

*The authors gratefully acknowledge the support of the SUTD Temasek Laboratories sponsored project Systems Technology for Autonomous Reconnaissance & Surveillance (STARS) and the SUTD-MIT International Design Center (http://idc.sutd.edu.sg).

Authors are with the Singapore University of Technology and Design, Engineering Product Development Pillar, 8 Somapah Road, Singapore 487372.

In this paper, we will present the operation principle for our LPMR where the vibrations of legs are similar to the bounding gait locomotion of animals. The design and the fabrication will be presented and an operational prototype will be shown. An experimental characterization for the LPMR in terms of speed versus applied voltage, speed versus embedded mass and blocking force for different applied voltages will be given. At the end, a tether-less LPMR featuring a full suite of onboard electronics is demonstrated in this paper.

II. Operational Principle of the LPMR

The LPMR consists of unimorph piezoelectric actuator that acts both as the base body and the excitation source and two legs attached to it by contact joints as shown Fig.1. The piezoelectric patch is polarized in the thickness direction and the applied electric field is parallel to the polarization direction; therefore, a periodic up and down bending motion will occur when an alternating sinusoidal voltage is applied to the piezoelectric patch. The legs are used to propel the LPMR forward and backward using the frictions between the legs tips and the support. Inspired from ultrasonic motors [6], [33], specific asymmetrical legs positions are determined to achieve forward and backward motion at the first and the second bending modes of vibrations respectively. To move the LPMR towards the right (left), the legs should be positioned to the left (right) of the antinodes of the bending modes of vibrations. Fig. 2 shows the first and second bending modes of vibrations for free-free beam where the solid rectangles and dashed rectangles represent the possible locations of legs to propel the LPMR at the first resonant frequency (f_1) towards the right and at the second resonant frequency (f_2) towards the left respectively.

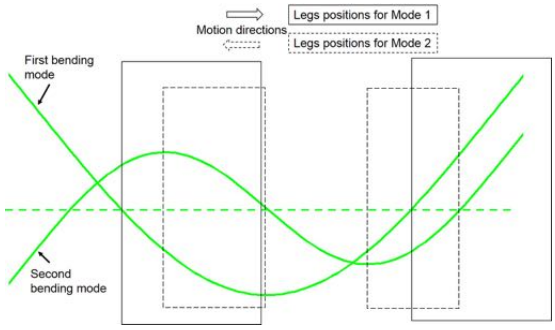

Fig. 2. Legs positions for the LPMR at f_1 & f_2

Hence as long as the legs are positioned within the intersection between the solid and dashed rectangles, the LPMR achieves forward and backward motion at the first and second resonant frequency respectively. The legs are supposed to be rigid, i.e. the frequencies of the bending vibrations modes are much smaller than the first natural frequency of the legs. For a configuration where the legs are positioned within the intersection between the solid and dashed rectangles, the corresponding vibrations of legs at f_1 & f_2 when applying an alternating sinusoidal voltage are shown in Fig. 3. For clarification, the vibrations of the elastic body are exaggerated on the Fig. 3.

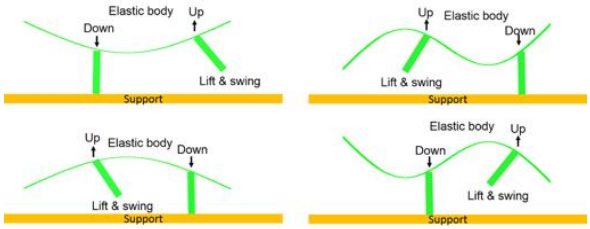

Fig. 3. Legs vibrations at f_1 (left) & f_2 (right) for the maximum (top) & minimum (bottom) applied voltage

Based on the legs motion due the the nodal vibrations given in Fig. 3, a visual illustration of the bidirectional locomotion technique is shown in Fig. 4 during one complete vibrtaion period T. This illustration has been depicted without the deformation of the elastic body. From Fig. 4, the LPMR lands with one leg and brings the other leg in the direction of motion to achieve one leg step on a half period $T/2$. Then in the next half period, the legs switch their roles for the next leg step. This locomotion technique is known for animals as the bounding gait locomotion which is a form of legged locomotion generally observed when a quadruped animal is running at the highest speed. In the next section, the design and the fabrication of the LPMR will be presented.

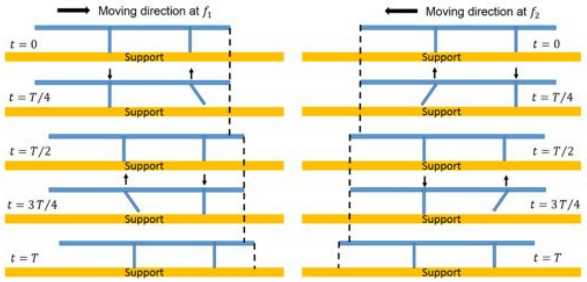

Fig. 4. Visual illustration of bidirectional locomotion at f_1 (going forward/right) & f_2 (going backward/left) during one period T

III. Design and Fabrication of the LPMR

A. Design

Based on the dimensions of commercially available piezoelectric patch, the *NCE*53, soft *PZT* from Noliac Inc. was chosen to be the active layer of the unimorph actuator due to the size range available. Next, Aluminium was chosen as the passive layer of the unimorph actuator due to its efficient electromechanical conversion [34]. Both the *PZT* and Aluminum have similar dimensions except for thickness, where it was chosen differently to obtain the maximum electromechanical conversion from the piezoelectric material as a composite structure. For this desing, the Aluminium thickness was chosen to be two times the thickness of the

PZT [34]. Table I gives the properties and the geometric parameters for the LPMR.

TABLE I

PROPERTIES AND GEOMETRY OF THE PZT AND THE ALUMINIUM LAYER

Properties, geometry	$PZT(p)$	Aluminium (m)
$c_m(Pa)$	-	69×10^9
$\rho_p,\rho_m(kg.m^{-3})$	7600	2700
$d_{31}(m.V^{-1})$	-1.5×10^{-10}	-
$S_{11}(Pa^{-1})$	1.6×10^{-11}	-
$l_p,l_m\times b\times t_p,t_m(mm^3)$	$50\times10\times0.5$	$50\times10\times1$

As shown in section Section II, the LPMR moves forward and backward at the first and second resonant frequency for the piezoelectric unimorph actuator (f_1, f_2) respectively which are the operating frequency for the LPMR. The resonant frequencies in case of free-free piezoelectric unimorph actuator is determined in (1).

$$f_n = \frac{(\beta_n l)^2}{2\pi l^2}\sqrt{\frac{(cI)_{eq}}{(\rho A)_{eq}}} \tag{1}$$

where $(cI)_{eq}$ and $(\rho A)_{eq}$ are the equivalent flexural rigidity and the equivalent mass per unit length of the piezoelectric unimorph actuator as defined by

$$(cI)_{eq} = (I_p c_p + I_m c_m), \tag{2}$$

$$(\rho A)_{eq} = b(\rho_p t_p + \rho_m t_m), \tag{3}$$

where ρ_p and ρ_m are the volume densities for the piezoelectric and aluminium layers respectively and the numerical values are given in Table I, I_m and I_p are the moments of inertia for the piezoelectric and aluminium layers cross section respectively and they are given in [35], β_n is the wavenumber and it is determined in [35] for free-free boundary conditions and l is the length of the piezoelectric unimorph actuator and it is given in Table I. Using (1), the analytical operating resonant frequencies f_1 & f_2 for the LPMR were found to be 2.4 kHz & 6.7 kHz respectively. However, our goal is to achieve forward and backward motion at a frequency below 3.2 kHz which is the frequency bandwidth for the micro piezoelectric driver that will be used later in the paper to power the piezoelectric unimorph actuator. A possible solution is to achieve forward motion at the first resonant frequency (f_1) and backward motion at a frequency between the two modes ($f_1 < f < f_2$).

The legs positions are determined using the mode shapes (bending modes of vibrations) of the piezoelectric unimorph actuator as discussed in section II and Fig. 2, where they are determined by the intersection between the solid and dashed rectangles. The simulation results for normalized modes shapes at f_1 & f_2 for the chosen design for the piezoelectric unimorph actuators are shown in Fig. 5 where the possible locations of legs are marked within the rectangles. Analytical equations for the mode shapes in case of free-free piezoelectric unimorph actuator can be found in [35]. Readers can refer to [6], [35], [36], [37], [38], for more details about modelling of piezoelectric-metal composite beams.

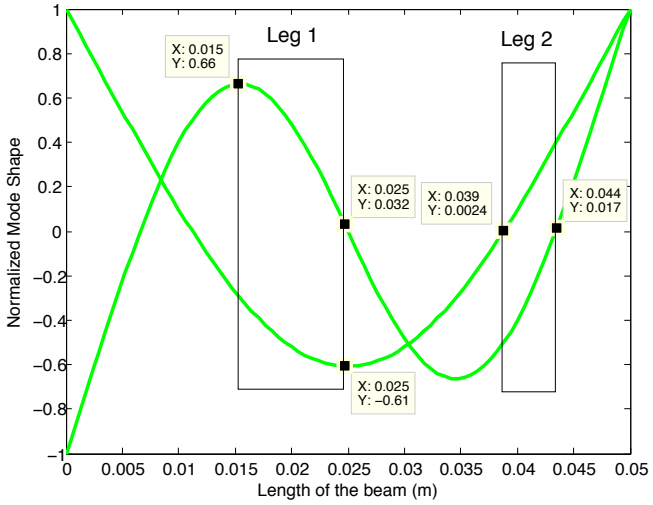

Fig. 5. Mode shapes and legs positions at f_1 & f_2 for the piezoelectric unimorph actuator

From Fig. 5, the legs can be placed anywhere between the rectangles to achieve forward and backward motion at f_1 & f_2 respectively. Leg 1 can be between 15 *mm* and 25 *mm* and Leg 2 can be between 39 *mm* and 44 *mm*. The location of Leg 2 is more sensitive when working between the two modes ($f_1 < f < f_2$) than the location of Leg 1 which is almost unaffected. As seen in Fig. 2, the range of intersection between the solid (f_1) and dashed (f_2) rectangles is small for Leg 2 and it is included in the solid rectangle (f_1) for Leg 1. Therefore, to achieve forward motion at the first mode (f_1) and backward motion between the two modes ($f_1 < f < f_2$); Leg 1 is remained at its place and Leg 2 is pushed toward the end of the piezoelectric unimorph actuator. Leg 1 is chosen to be at 20 *mm* and Leg 2 is placed at 45 *mm*. The legs are made from steel which has higher stiffness than the piezoelectric unimorph actuator with 9 *mm* length and 1 *mm* thickness.

B. Fabrication

A third leg with 7 *mm* length (2 *mm* shorter) is added at 7 *mm* from the end of the beam length. This Leg doesn't touch the ground and therefore does not play a role in locomotion. Its role, however, is to prevent the LPMR from tipping over when the power is switched off. This is especially important when the LPMR carries heavy payloads, where the LPMR is in the risk of breaking. Fig. 6 shows the experimental prototype of the LPMR without powering electronics. Three contact joints as shown Fig. 6 are bonded onto the aluminium beam using a strong bonding epoxy adhesive (two parts Araldite epoxy). The legs are connected to the aluminium beam at the desired points computed above via the contact points. Then, the chosen piezoelectric patch is bonded onto the aluminium beam using the same epoxy and thin wires are soldering on the piezoelectric patch electrodes.

IV. EXPERIMENTAL INVESTIGATION

To validate and verify the forward and backward resonant frequencies, a signal generator is used to generate a refer-

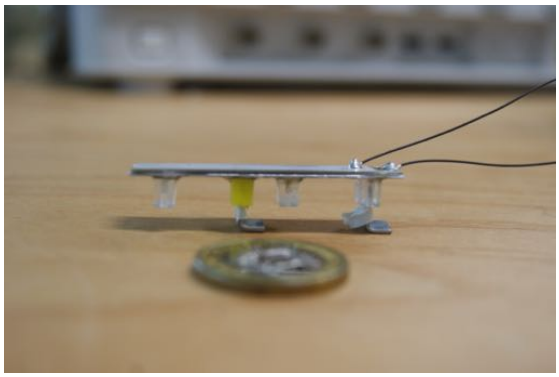

Fig. 6. Mechanical structure of the experimental LPMR

ence sinusoidal voltage to the piezoelectric driver *PDu*100 from PiezoDrive inc. and the subsequent amplified voltage powers the piezoelectric patch on the LPMR. Through direct experiments, the LPMR shows forward motion at 2.4 *kHz* and backward motion at 3.1 *kHz*, which are both below the limit of the micro piezoelectric driver. The bounding gait locomotion as described in section II, Fig. 4 is also verified using a slow motion capture system. Thereafter, an experimental characterization for the LPMR in terms of speed versus applied voltage, speed versus embedded mass and blocking force for different applied voltages is done and results are given in Fig. 7, Fig. 8 and Fig. 9. At

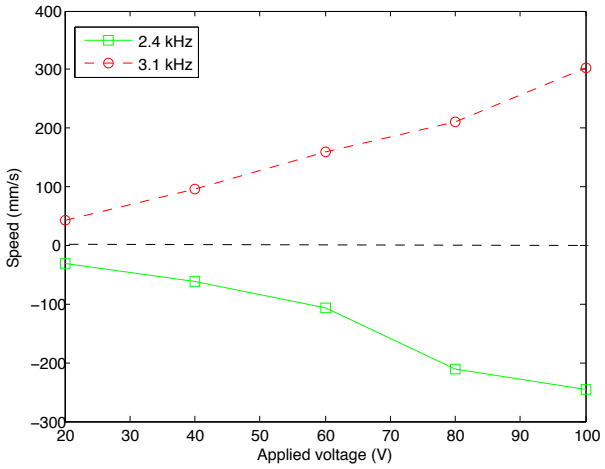

Fig. 7. Speed of the LPMR versus applied voltage

constant conditions (frequency, voltage & embedded mass), the speed is measured three times using the formula d/t and the average value is token. Also, at constant conditions, the blocking force is measured using an inclined plane when the speed of the LPMR becomes zero. The blocking force is important to determine the nominal operating point for the LPMR. It is the maximum force generated by the LPMR and it is measured experimentally on an inclined plane when the speed of the LPMR becomes zero. Some experimental tests for the LPMR are shown in Fig. 10. The power consumption of the LPMR is analytically computed using (4) and results

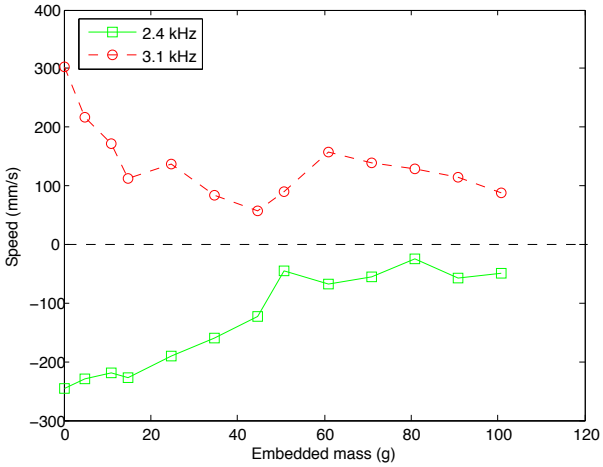

Fig. 8. Speed of the LPMR versus embedded mass at 100 V amplitude

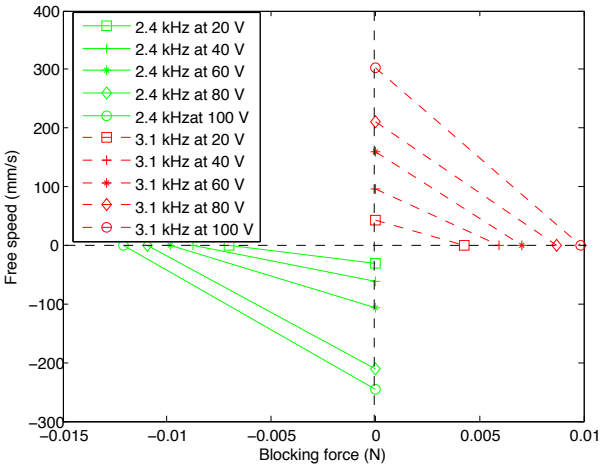

Fig. 9. Free speed & blocking force for the LPMR

are given in Fig. 11.

$$1/2fCV^2 \tag{4}$$

Where f is the applied frequency, C is the capacitance of the piezoelectric patch and V is the applied voltage. At 100 V amplitude, the LPMR consumes 0.17 W and 0.22 W for forward and backward motion respectively.

V. A REMOTE CONTROLLED LPMR

A control architecture for the LPMR is given in Fig. 12. The electronic circuit design and the interface design for the LPMR are given in Fig. 13 and Fig. 15 respectively. A chassis cover is designed and 3D printed to cover the LPMR body and the onboard electronics. A figure for the chassis cover is given in Fig. 15. Fig. 16 shows the LPMR with the chassis cover, a battery and the onboard electronics. An image sequence of the remote controlled LPMR moving on a wood substrate at 2.4 kHz (forward motion) and 3.1 kHz (backward motion)is shown in Fig. 17.

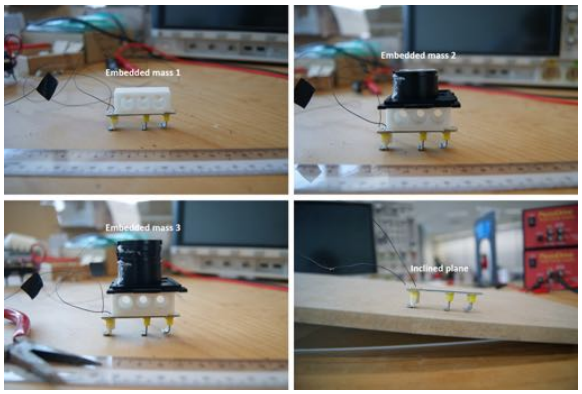

Fig. 10. Experimental tests

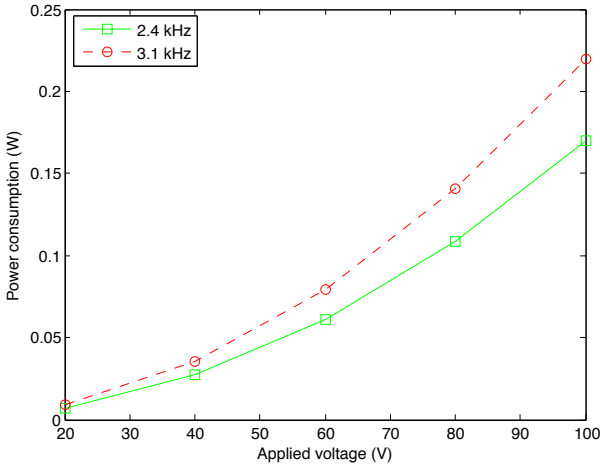

Fig. 11. Power consumption for the LPMR

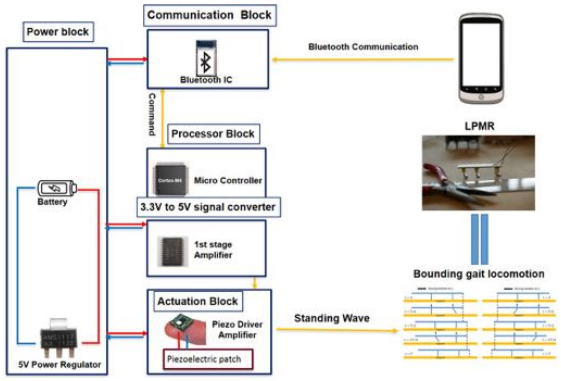

Fig. 12. Control architecture for the LPMR

VI. Conclusion

In this paper, we illustrated the design and manufacturing process for tether-less Legged Piezoelectric Miniature Robot (LPMR) where only one piezoelectric patch is used. Basing on the bending modes of vibrations, a bidirectional motion is achieved by choosing specific positions for the legs where the vibrations of legs were similar to the bounding gait locomotion of animals. The LPMR showed high performance in terms of speed and load carried. The onboard electronics presented in this paper will be miniaturized in future work.

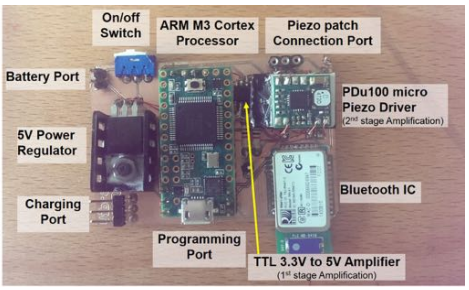

Fig. 13. Electronic circuit design for the LPMR

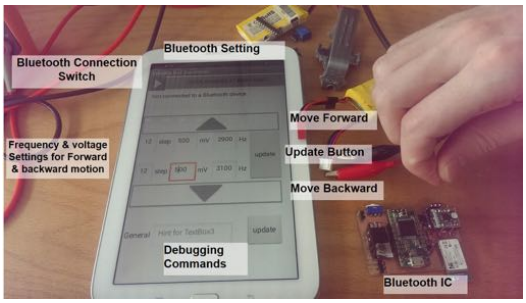

Fig. 14. Interface design for the LPMR

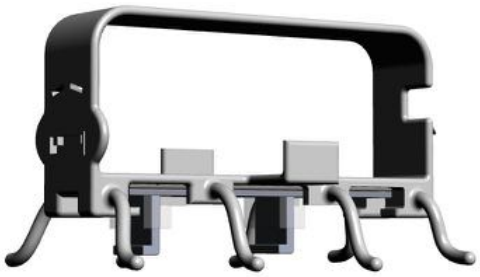

Fig. 15. Chassis cover for the LPMR

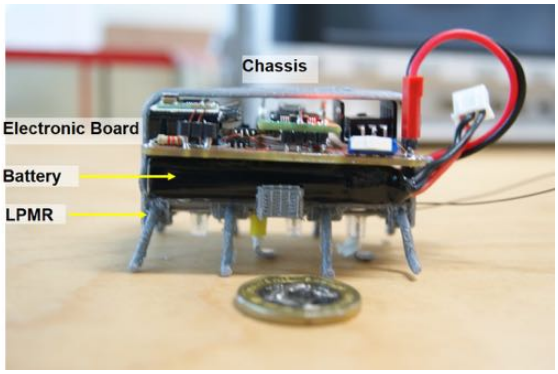

Fig. 16. The complete prototype of the LPMR

References

[1] K. Uchino, "Expansion from IT/Robotics to ecological/energy applications", ACTUATOR 2006, p.48, 2006.

[2] T. Ebefors and G. Stemme, "Microrobotics" in The MEMS Handbook (M. Gad-el Hak,ed.), pp. 28.1, Boca Raton, FL: CRC Press, 2005.

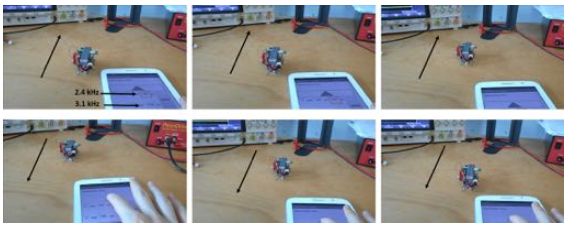

Fig. 17. An image sequence of the remote controlled LPMR

[3] J.B.Penella, "Smart material for microrobotics. Motion, control and power harvesting". Phd thesis, Barcelona university, Spain, 2005.

[4] A. Codourey, W. Zesch, R. Buchi, and R. Siegwart, "A robot system for automated handling in micro-world" in Proc. IEEE/RSJ Int. Conf. on Intelligent Robots and Systems, IROS 95, vol. 3, pp. 185, 1995.

[5] A. Torii, H. Kato, and A. Ueda, "A miniature actuator with electromagnetic elements" Electrical Engineering in Japan (English translation of Denki Gakkai Ronbunshi), vol. 134, no. 4, pp. 70, 2001.

[6] K. J. Son, V. Kartik, J. A. Wickert, and M. Sitti, "An ultrasonic standing-wave-actuated nano-positioning walking robot: Piezoelectric-metal composite beam modeling" Journal of Vibration and Control, vol. 12, no. 12, pp. 1293, 2006.

[7] S.I. Aoshima, T. Tsujimura, and T. Yabuta, "Miniature mobile robot using piezo vibration for mobility in a thin tube" Journal of Dynamic Systems, Measurement and Control, Transactions of the ASME, vol. 115, no. 2 A, pp. 270, 1993.

[8] S. Heo, T. Wiguna, H.C. Park, N.S.Goo, "Effect of an Artificial Caudal Fin on the Performance of a Biomimetic Fish Robot Propelled by Piezoelectric Actuators", Journal of Bionic Engineering 4, pp. 151, 2007.

[9] G. Kosa, P. Jakab, N. Hata, F. Jolesz, Z. Neubach, M. Shoham, M. Zaaroor, G. Szekely "Flagellar swimming for medical micro robots: Theory, experiments and application", 2nd IEEE RAS & EMBS International Conference on Biomedical Robotics and Biomechatronics, pp. BioRob 2008.

[10] S. H. Suhr, Y. S. Song, S. J. Lee and M. Sitti, "Biologically Inspired Miniature Water Strider Robot," Proceedings of the Robotics: Science and Systems I, Boston, U.S.A., pp. 319. 2005.

[11] M. Sitti, "PZT actuated four-bar mechanism with two flexible links for micromechanical flying insect thorax", Proceedings ICRA. IEEE International Conference on Robotics and Automation, vol.4, pp. 3893, 2001.

[12] J. M. Breguet, S. Johansson, W. Driesen, U. Simu, "A review on actuation principles for few cubic millimetre sized mobile microrobots", Proceedings of the 10th International Conference on New Actuators, pp. 374, 2006.

[13] Y. K. Yong, A. J. Fleming "Piezoelectric Actuators with Integrated High Voltage Power Electronics". Mechatronics, IEEE/ASME Transactions on, Volume:20, Issue:2, pp. 611, 2014.

[14] M. Karpelson, G. Y. Wei, R. J. Wood "Driving high voltage piezoelectric actuators in microrobotic applications". Sensors and Actuators A: Physical, 2011.

[15] Chi hsiang pan. Sz sheng tzou, Ruei yang shiu "A Novel Wireless and Mobile Piezoelectric Micro Robot", Proceedings of the 2010 IEEE International Conference on Mechatronics and Automation, August 4 - 7, Xi'an, China, 2010.

[16] Ranjana Sahai, Srinath Avadhanula, Richard Groff, Erik Steltz, Robert Wood, and Ronald S. Fearing, "Towards a 3g Crawling Robot through the Integration of Microrobot Technologies" Proceedings of the 2006 IEEE International Conference on Robotics and Automation, Orlando, Florida - May 2006.

[17] Michael Goldfarb, Michael Gogola, Gregory Fischer and Ephrahim Garcia, "Development of a piezoelectrically-actuated mesoscale robot quadruped", Journal of Micromechatronics, Volume 1, Issue 3, pp. 205, 2001.

[18] Thanhtam Ho, Sangyoon Lee, "Implementation of a piezoelectrically actuated self-contained quadruped robot", Proc. SPIE 7332, Unmanned Systems Technology XI, 73320E, 30 April 2009.

[19] Anh Tuan Nguyen and Sylvain Martel, "A New Actuation Mechanism Based on a Synchronized Vibrating Platform for Micro and Nanofactories", 5th International Workshop on Microfactories, 2006.

[20] Anh Tuan Nguyen and Sylvain Martel, "Miniaturization of a Piezo-Actuation System Embedded in an Instrumented Autonomous Robot", IEEE North-East Workshop on Circuits and Systems, 2006.

[21] F.De Ambroggi, L. Fortuna, G. Muscato, "PLIF: Piezo Light Intelligent Flea new micro-robots controlled by self-learning techniques", Proceedings of IEEE International Conference on Robotics and Automation, 1997.

[22] Giovanni Muscato, "The Collective Behaviour of Piezoelectric Walking Microrobots: Experimental Results", Journal of Intelligent Automation & Soft Computing, 2013.

[23] Thanhtam Ho, Sunghac Choi, Sangyoon Lee, "Development of a Biomimetic Quadruped Robot", Journal of Bionic Engineering 4, pp. 193, 2007.

[24] Abdul A. Yumaryanto, Jaebum An, Sangyoon Lee, "A Cockroach-Inspired Hexapod Robot Actuated by LIPCA", IEEE Conference on Robotics, Automation and Mechatronics, 2006.

[25] Minami Takato, Masaki Tatani, Hirozumi Oku, Yuki Okane, Junichi Tanida, Shinpei Yamasaki, Ken Saito and Fumio Uchikoba, "A Millimetre-sized Robot Realized by a Piezoelectric Impact-type Rotary Actuator and a Hardware Neuron Model", International Journal of Advanced Robotic Systems, 2014.

[26] Dragan Avirovik, Bryan Butenhoff and Shashank Priya, "Millipede-inspired locomotion through novel U-shaped piezoelectric motors", Smart Mater. Struct. 23, 2014.

[27] Andrew Thomas Baisch, "Design, Manufacturing, and Locomotion Studies of Ambulatory Micro-Robots", PhD thesis, Harvard University, Cambridge, Massachusetts, 2013.

[28] Shannon A. Rios, Andrew J. Fleming and Yuen Kuan Yong, "Design of a Two Degree of Freedom Resonant Miniature Robotic Leg", IEEE International Conference on Advanced Intelligent Mechatronics, 2015.

[29] N. Lobontiu, M. Goldfarb, E. Garcia, "A piezoelectric-driven inchworm locomotion device", Journal of Mechanism and Machine Theory 36, pp. 425, 2001.

[30] F. Becker, V. Minchenya, K. Zimmermann and I. Zeidis,"Single Piezo Actuator Driven Micro Robot for 2-Dimensional Locomotion", Micromechanics and Microactuators, Springer, 2012.

[31] F. Becker, V. Minchenya, I. Zeidis and K. Zimmermann, "modeling and dynamical simulation of vibration-driven robots", 56th international scientific colloquium, Ilmenau University of Technology, Germany, 12 September 2011.

[32] F. Becker and K. Zimmermann, "Piezo-driven Micro Robots for Different Environments: Prototypes and Experiments", ROBOTIK 2012.

[33] S. He, W. Chen, X. Tao and Z. Chen, Standing wave bi-directional linearly moving ultrasonic motor. IEEE Transactions on Ultrasonics, Ferroelectrics and Frequency Control, 45(5), pp. 1133, 1998.

[34] H. Hariri, Y. Bernard, and A. Razek, "A traveling wave piezoelectric beam robot". Smart Materials and Structures, 23(2), 2013.

[35] H. Hariri, Y. Bernard, A. Razek, "Analytical and finite element model for unimorph piezoelectric actuator: Actuator design??. Proceedings of Piezo2011, pp. 71, 2011.

[36] R.G. Ballas, "Piezoelectric multilayer beam bending actuator". Springer, 2007.

[37] Q. M. Wang, L. E. Cross, "Performance analysis of piezoelectric cantilever bending actuators Ferroelectrics", pp. 187, 1998.

[38] N. Jalili, "Piezoelectric-Based Vibration Control, From Macro to Micro-Nano Scale Systems", Springer, 2009.